HHS Public Access

Author manuscript

Inhal Toxicol. Author manuscript; available in PMC 2023 November 20.

Published in final edited form as:

Inhal Toxicol. 2023 ; 35(9-10): 241–253. doi:10.1080/08958378.2023.2224394.

Biological effects of inhaled crude oil vapor. III. Pulmonary inflammation, cytotoxicity, and gene expression profile

Tina M. Sager,

Pius Joseph,

Christina M. Umbright,

Ann F. Hubbs,

Mark Barger,

Michael L. Kashon,

Jeffrey S. Fedan,

Jenny R. Roberts

Health Effects Laboratory Division, National Institute for Occupational Safety and Health, Morgantown, WV, USA

Abstract

Objective: Workers may be exposed to vapors emitted from crude oil in upstream operations in the oil and gas industry. Although the toxicity of crude oil constituents has been studied, there are very few *in vivo* investigations designed to mimic crude oil vapor (COV) exposures that occur in these operations. The goal of the current investigation was to examine lung injury, inflammation, oxidant generation, and effects on the lung global gene expression profile following a whole-body acute or subchronic inhalation exposure to COV.

Materials and Methods: To conduct this investigation, rats were subjected to either a whole-body acute (6 hr) or a sub-chronic (28 d) inhalation exposure (6 hr/d × 4 d/wk × 4 wk) to COV (300 ppm; Macondo well surrogate oil). Control rats were exposed to filtered air. One and 28 d after acute exposure, and 1, 28, and 90 d following sub-chronic exposure, bronchoalveolar lavage was performed on the left lung to collect cells and fluid for analyses, the apical right lobe was preserved for histopathology, and the right cardiac and diaphragmatic lobes were processed for gene expression analyses.

Results: No exposure-related changes were identified in histopathology, cytotoxicity, or lavage cell profiles. Changes in lavage fluid cytokines indicative of inflammation, immune function, and endothelial function after sub-chronic exposure were limited and varied over time. Minimal gene expression changes were detected only at the 28 d post-exposure time interval in both the exposure groups.

CONTACT Tina M. Sager sst2@cdc.gov Toxicology and Molecular Biology Branch, National Institute for Occupational Safety and Health, 1000 Frederick Lane, Morgantown, WV 26508, USA.

Disclosure statement

No potential conflict of interest was reported by the author(s). The findings and conclusions in this report are those of the authors and do not necessarily represent the official position of the National Institute for Occupational Safety and Health, Centers for Disease Control and Prevention. Mention of brand name does not constitute product endorsement.

Conclusion: Taken together, the results from this exposure paradigm, including concentration, duration, and exposure chamber parameters, did not indicate significant and toxicologically relevant changes in markers of injury, oxidant generation, inflammation, and gene expression profile in the lung.

Keywords

Crude oil vapor; pulmonary toxicity; gene expression; inflammation; lung; rats

Introduction

This is the third study in a series of tandem papers that focuses on examining toxicity following *in vivo* inhalation exposure to crude oil vapor (COV) in upstream oil operations (McKinney et al. 2022; Fedan 2023). Crude oil is a complex mixture of chemicals consisting primarily of normal alkanes and hydrocarbons. The hydrocarbons are structurally defined in three groups as aromatic, naphthenic or cycloparaffinic (cycloalkanes or naphthenes), and aliphatic/paraffinic (alkanes) compounds that exist in gaseous, liquid, and solid form, and which contain low concentrations of sulfur, nitrogen, and oxygen compounds and trace amounts of metal-containing components (Hawley 1981; IARC 1989; Lin and Tjeerdema 2008). The aromatic hydrocarbon group contains some of the most toxic constituents of crude oil including benzene and its derivatives, naphthalenes, phenanthrenes, pyrenes, xylenes, and toluene. Benzene, toluene, ethylbenzene, and xylenes, referred to as BTEX, are frequently measured together to represent the VOC fraction of COV exposure, as well as other exposures that may contain VOCs (ATSDR 2004).

The pulmonary and systemic toxicities induced by many of the individual vapor components of COV following inhalation exposure are well documented and are extensively reviewed (ATSDR 1995, 1999a, 1999b, 2005, 2007a, 2007b, 2010, 2017; Mckee et al. 2015). There are also a number of *in vivo* and *in vitro* pulmonary studies that examine various synthetic combinations of BTEX and other aliphatic and/or aromatic combinations of hydrocarbons as well (reviewed in ATSDR 2004; Carrillo et al. 2013; Fischäder et al. 2008; Khalil and Nasir 2010; Wang et al. 2014). In general, exposures to BTEX have been associated with cancers, (blood, kidney, lung, and liver), and non-cancerous toxicity including effects on central nervous system depression, respiratory diseases, kidney, liver, immune, and reproductive effects (ATSDR 2004, 2007a, 2007b, 2010, 2017; Chen et al. 2016).

Worker exposure to COV and related health effects was reviewed in Fedan (2023). Workers can be exposed to COV in upstream operations in the oil industry, as well as in clean-up operations following spills. Upstream activities where exposures can occur include exploration, drilling, transporting, and storage (Esswein et al. 2014a; Harrison et al. 2016; Retzer et al. 2018; Verma et al. 2000). Numerous cross-sectional studies focused on cancer incidence and mortality have been conducted with workers in the oil industry, but few have focused on upstream workers, and those that have report variable findings with some showing no observed increases and others showing increased incidence in melanoma (attributed to ultraviolet light exposure), mesothelioma (attributed to asbestos exposure), and acute myelogenous leukemia (attributed to benzene exposure) (Divine and

Barron 1987; Schnatter et al. 1992; Sathiakumar et al. 1995; Divine and Hartman 2000; Wong and Raabe 2000; Stenehjem et al. 2014). In addition to injuries and musculo-skeletal problems, respiratory disease was also commonly reported in a study of oil rig workers (Valentic et al. 2005). Acute severe respiratory and cardiovascular toxicity can also occur. Improperly opening of the hatch on top of a petroleum storage tank can result in the release of HCV/VOC plumes (>100,000 ppm). leading to worker exposure at or downwind from the storage tank (Jordan 2015; NIOSH 2015). The National Institute for Occupational Safety and Health (NIOSH 2015) reported nine sudden deaths caused by inhalation of hydrocarbon gases and vapors and oxygen deficiency among oil and gas extraction workers from January 2010 to March 2015.

A larger number of studies have assessed health effects in workers involved in oil spill clean-up operations elsewhere and from these, insights into the toxicity of COV can be gleaned. D'Andrea and Reddy (2014), reviewed numerous health effects studies from several large spills including *Exxon Valdez, MV Braer, Sea Empress, Erika, Prestige, Tasmin Spirit, Hebei Spirit*, and *Deepwater Horizon*. Commonly reported health effects included eye, nose, and throat irritation, upper and lower respiratory problems, headache, nausea/vomiting/diarrhea, dermatitis, fatigue, and psychological effects.More recent studies related to the Deepwater Horizon spill, with approximately 200 million gallons of oil spilled and tens of thousands of individuals involved in clean up operations including Coast Guard personel, other government personel, oil industry workers, Gulf coast residents and volunteers from around the United States (U.S. Coast Guard 2011; Kwok et al. 2017). Studies found acute respiratory symptoms (shortness of breath and wheezing) in Coast Guard personnel (Alexander et al. 2018), and long-term effects in oil spill clean-up workers included persistent or worsened hematologic (reduced blood platelets and increased hematocrit and hemoglobin), hepatic (increased blood liver enzymes), pulmonary (including chronic rhinosinusitis and lung function abnormalities), and cardiac (abnormal ECG results and ventricular hypertrophy) effects (D'Andrea and Reddy 2018).

Based on the results of the studies detailed above, a battery of inhalation studies was performed to assess different crude oil exposure paradigms *in vivo*. The oil used in this study was collected from the Macondo well, close to the site of the Deep Water Horizon Macondo Well blow-out in the Gulf of Mexico in 2010. Specifically, male rats were exposed to air or COV (300 ppm) for 6h × 1d (acute) or 6 h/d × 4 d/wk × 4 wks (sub-chronic). This battery of studies assessed pulmonary, cardiovascular, nervous, and immune system effects. The current study relates directly to several other studies in the battery. These studies found some alterations in lung function, including changes in basal airway resistance and an inhibitory effect of the airway epithelium on reactivity to methacholine (MCh). Acute COV exposure did not affect basal airway epithelial ion transport. However, the sub-chronic COV exposure facilitated alterations in active and passive ion transport (Fedan et al. 2022). Additionally, the cardiovascular assessment found that acute and subchronic exposure to COV led to alterations in the expression of NO synthases and antioxidant enzymes that regulate inflammation and oxidative stress in the heart and kidneys. Exposure also produced changes in arterial and diastolic blood pressure were noted in the acute exposure. (Krajnak et al. 2022). The neurological effects COV exposure included reductions in norepinephrine (NE), epinephrine (EPI), dopamine (DA) in dopaminergic brain regions, striatum, and midbrain

and large increase in and serotonin (5-HT) in the striatum Upregulation of synaptic and Parkinson's disease-related proteins in the striatum and midbrain were also found (Sriram et al. 2022). The immunotoxicity assessment of COV exposure found that COV exposure resulted in alterations in cellularity of phenotypic subsets that could impair immune function in rats (Weatherly et al. 2022).

To complement the above studies, the goal of the current study was to further examine the effects of whole-body COV inhalation exposure on the lung. The toxicology profile in this study focused primarily on lung histopathology, cytotoxicity, oxidant generation, inflammation, and gene expression. Because changes in lung function were found and systemic effects related to inflammation and oxidant balance were observed, we hypothesized that the exposure may lead to lung pathology and molecular changes related to increased inflammation and oxidative stress in the lung. To address this we examined these end points using the identical acute and sub-chronic exposure scenarios described above.

Methods

Animals

All animal studies were conducted in facilities accredited by AAALAC International, were approved by the Institutional Animal Care and Use Committee (protocols 13-JF-R-014, 14-JF-R-011 and 16-JF-R-020 v. 3 and v. 4) and were in compliance with the Public Health Service Policy on Humane Care and Use of Laboratory Animals and the NIH Guide for the Care and Use of Laboratory Animals. Male Sprague-Dawley rats ([H1a: (SD) CVF, approximate body weight of 200–275 g at arrival], were obtained from Hilltop Lab Animals, Inc. (Scottdale, PA). All animals were free of viral pathogens, parasites, mycoplasm, *Heliobacter* and cilia-associated respiratory bacillus. Animals were acclimated for one week and housed in ventilated micro-isolator units supplied with HEPA-filtered laminar flow air (Lab Products OneCage; Seaford, DE), with Teklad Sanichip and Teklad Diamond Dry cellulose bedding (Watertown, TN). They were provided tap water and autoclaved Teklad Global 18% protein rodent diet (Harlan Teklad; Madison, WI, USA) *ad libitum*. Rats were housed in pairs under controlled light cycle (12 h light/12 h dark) and temperature (22–25 °C) conditions.

COV exposure

The crude oil used in this investigation was provided by BP Exploration and Production, Inc. and was characterized in McKinney et al. (2022). The oil is reference material associated with the 2010 Deepwater Horizon spill from the Macondo Well in Mississippi Canyon Block 252, i.e. "surrogate oil" that is similar to the Macondo Well crude oil. The target exposure and concentration were total VOCs at 300 ppm, for the two different exposure durations in a whole-body inhalation system. In addition to continual monitoring of total VOCs throughout the exposure duration each day, BTEX was also measured during exposure. The exposure system is described in detail in McKinney et al. (2022). Briefly, a computer-controlled custom system and chamber were developed which injected a heated flow of oil into a collision atomizer. Filtered air was combined with the atomized oil and mixed in a column then passed through a HEPA filter to remove oil droplets. Several control runs

were conducted to establish the flow rate that generated 300 ppm total VOC (COV) in the exposure chamber. The whole-body exposure chamber itself was airtight with stainless steel inflow and exhaust tubes. Animals were housed in the chamber in stainless steel chamber racks with no bedding as described in McKinney et al. (2022). Control animals were exposed to filtered air in a separate and identical exposure system/chamber. The COV level used in the animal exposures falls within the range of those that have been measured in upstream operations in the oil and gas industry (NIOSH 2015). Its physical and chemical properties are described in McKinney et al. (2022).

Rats were exposed by whole-body inhalation to 300 ppm of COV aerosol for 6 hr/d during the light cycle for one of two durations: the acute exposure was one day, and the sub-chronic exposure was 4 d/wk for 4 consecutive weeks. Control animals were simultaneously exposed to filtered air and were otherwise handled similarly. During their 6-h inhalation exposure(s) to air or COV, the rats were not provided with food or water. The exposure chamber and conditions during the inhalation exposure of the rats were as described in McKinney et al. (2022). For the acute exposure, there was an $n = 8$ for the air group and an $n = 8$ for the COV group at each time point for a total of 32 rats. For the sub-chronic exposure, there was also an $n = 8$ for the air group and an $n = 8$ for the COV group at each time point for a total of 48 rats.

Collection of biospecimens

Samples were collected from animals at 1or 28 d following the 1-d acute COV-exposure, or 1, 28, and 90 d following the last day of the 4-week sub-chronic COV exposures. The control and COV-exposed rats were euthanized by an over-dose of sodium pentobarbital (100–300 mg/kg, i.p.; Fatal Plus; Vortec Pharmaceuticals, Dearborn, MI, USA) followed by exsanguination. The trachea was then cannulated, the chest cavity was opened, the right bronchi were clamped off, and bronchoalveolar lavage (BAL) was performed on the left lung (Sellamuthu et al. 2011).

The acellular fraction of the first lavage was obtained by filling the left lung with 3 ml of ice-cold phosphate-buffered saline (PBS), massaging for 30 sec, withdrawing, and repeating the process once. This concentrated aliquot was withdrawn, retained on ice, kept separate, and designated as the first fraction of BAL fluid (BALF). The subsequent aliquots were approximately 4 ml in volume, instilled once with light massaging, withdrawn, and combined until a 24 ml-volume was obtained. For each animal, both lavage fractions were centrifuged (10 min, 570 × *g*, 4 °C), the cell pellets were combined and re-suspended in 1 ml of PBS, and the acellular fluid from the first fraction was retained for further analysis.

Following lavage, the right lungs were unclamped, the cannulated trachea and right lung lobes (cardiac and diaphragmatic) were removed. The apical lobe was tied off and removed for gene expression analysis, the remaining lobes were pressure-fixed in 10% neutral buffered formalin by airway pressure fixation under 30 cm water pressure to total lung capacity for 15 min. Once the fixation process was complete, the lung lobes were paraffin-embedded, sectioned, and stained with hematoxylin and eosin (H&E). The apical lobe from the unlavaged right lung of the rats was cut into pieces and stored in RNA later (Invitrogen; Carlsbad, CA, USA) for RNA isolation as described below.

Lung histopathology

For histopathological analysis, H&E-stained sections of right lung tissue from animals in the sub-chronic study and corresponding controls were evaluated for morphologic alterations by a board-certified veterinary pathologist, at 1, 28, and 90 d following exposure. The evaluation included semi-quantitative scores of any potentially exposure-related morphologic alterations on a scale of 0–5, for distribution (0 = not observed, 1 = focal, 2= locally extensive, 3 = multifocal, 4= multifocal and coalescent, and 5 = diffuse) and severity (0= no observed effect, 1= minimal, 2= mild, 3= moderate, 4= marked, and 5 = severe (Hubbs et al. 1997).

Analysis of BALF lactate dehydrogenase (LDH) activity and cytokines levels

LDH activity in the acellular BALF of the rats exposed to filtered air or COV was measured to evaluate cytotoxicity as an index of lung injury following both exposure scenarios, and a protein panel was evaluated following the sub-chronic exposure. LDH activity was determined as described previously (Sellamuthu et al. 2011) in the first fraction of the acellular BALF. A battery of 27 proteins was evaluated in BALF samples from the sub-chronic exposure at 1, 28, and 90 d post-exposure using a commercially available multiplex assay as a broad screen for toxicity (Eve Technologies Corporation; Calgary, Canada.). This assay was selected as a discovery panel with proteins representing a broad range of responses in the lung including chemotaxis of white blood cells, inflammation, immune cell activation, and tissue remodeling. Granulocyte-colony stimulating factor (G-CSF), eotaxin, granulocyte-macrophage colony stimulating factor (GM-CSF), interferon (IFN)-γ,interleukin (IL)-1α, IL-1β, IL-2, IL-4, IL-5, IL-6, IL-10, IL-12 (p70), IL-13, IL-17A, IL-18, IP-10 [IFN-γ-inducible protein (IP)-10], neutrophil activating protein CXCL1 (GRO/KC), fraktalkine, leptin, epidermal growth factor (EGF), epithelial-derived neutrophil-activating peptide 78 (LIX), macrophage chemotactic protein (MCP)-1, monocyte inflammatory protein (MIP)-1α, MIP-2, regulated on activation normal T-cell expressed and secreted (RANTES), tumor necrosis factor (TNF)-α, and vascular endothelial growth factor (VEGF)-A were assessed. Additionally, the following proteins were also evaluated by enzyme-linked immunosorbent assay (ELISA) to further add to the discovery panel: cholecystokinin (CCK or CCL28), IL-27, IL-35 and TGF-β.

Cell differentials: alveolar macrophages (AMs)/monocytes, neutrophils, and eosinophils

The total numbers of BAL cells collected from rats exposed to air or COV following both exposure scenarios were counted using a Coulter Multisizer II (Coulter Electronics; Hialeah, FL). Cell differentials were performed to determine the total number of AMs/monocytes, neutrophils, and eosinophils. Briefly, 10^5 cells from each rat were spun down onto slides with a Cytospin 3 centrifuge (Shandon Life Sciences International; Cheshire, England) and labeled with a Leukostat stain (Fisher Scientific; Pittsburgh, PA, USA) to differentiate cell types. A minimum of two hundred cells per slide were counted, and the percentages of AMs/monocytes, neutrophils, and eosinophils were multiplied by the total number of lavaged cells to calculate the total number of each cell type.

Oxidant generation by lung phagocytes

To estimate lung phagocyte oxidant production, a luminol-dependent chemiluminescence (CL) assay was performed on BAL cells as a measure of the light generated by the production of reactive oxygen species (ROS) by AM using a Berthold LB953 luminometer (Wallace Inc.; Gaithersburg, MD), as described previously (Antonini et al. 1994). Baseline oxidant production by the cells was measured in the absence of a stimulant. Luminol (Sigma-Aldrich; St. Louis, MO, USA) was used to enhance detection of the light, and 0.2 mg/ml of unopsonized zymosan (Sigma-Aldrich) was added to the assay immediately prior to the measurement of CL to activate the cells. Because rat neutrophils do not respond to unopsonized zymosan, the zymosan-stimulated CL produced is from AMs (Castranova et al. 1990). Measurement of CL was recorded for 15 min at 37 °C, and the integral of counts per minute (cpm) per 10^6 cells vs. time was calculated. CL was calculated as the cpm of the stimulated cells minus the cpm of the corresponding resting cells, and the value was normalized to total number of AM/monocytes in the BAL for zymosan-stimulated CL.

RNA isolation from lung samples

Total RNA, free of contaminating genomic DNA and proteins, was isolated from a piece of the lung tissue stored frozen in RNAlater for both acute and sub chronic COV exposed rat lungs, at the 1- and 28-d post-exposure time intervals. RNA isolation, including the optional on-column DNase digestion was conducted using the RNeasy Mini Kit (Qiagen, Inc.; Valencia, CA, USA) following the procedure provided by the manufacturer. The integrity and purity of the RNA samples isolated were determined using an Agilent 2100 Bioanalyzer (Agilent Technologies; Palo Alto, CA, USA). Total RNA was quantified by UV-Vis spectrophotometry. Only RNA samples exhibiting an RNA Integrity Number (RIN) ≥8.0 were used in the gene expression studies.

Determination of lung gene expression profile

Gene expression was evaluated following both acute and sub-chronic exposure to COV. One microgram total RNA/sample was used to create next generation sequencing (NGS) libraries using the Illumina TruSeq® Stranded Total RNA Library Prep kit (Illumina, Inc.; San Diego, CA) following the protocol provided by the manufacturer. Briefly, following depletion of ribosomal RNA (rRNA), the RNA samples were purified, fragmented (68 °C for 5 min), and primed for cDNA synthesis. The denatured and cleaved RNA fragments were purified using a bead cleanup procedure and reverse-transcribed into first strand cDNA using reverse transcriptase and random primers. While synthesizing the double stranded (ds) cDNA, dUTP was incorporated in place of dTTP followed by the addition of a single ‘A’ nucleotide to the 3 prime ends to facilitate proper adapter ligation to each sample. Indexing adapters were ligated to the ends of the ds cDNA. After adapter ligation, the samples were PCR amplified (12 cycles) to enrich the DNA fragments containing the adapter molecules and to enhance the amount of DNA in the library using a Veriti™ 96 Well Thermal Cycler (Applied Biosystems; Foster City, CA). The PCR amplified cDNA library samples were quantified using a dsDNA HS Assay Kit (Invitrogen by ThermoFisher Scientific; Waltham, MA) and Qubit 3.0 Fluorometer (Invitrogen by ThermoFisher Scientific). Average fragment size and fragment distribution of the cDNA library samples were then assessed using an Agilent 2100

Bioanalyzer (Agilent Technologies; Santa Clara, CA, USA) with High Sensitivity DNA Reagents (Agilent Technologies).

Individual sample libraries were sequenced by the Genome Sequencing Laboratory, Centers for Disease Control and Prevention (Atlanta, GA) for 2 × 75 base pair, paired-end sequencing using an Illumina HiSeq 2500 machine in rapid run mode using HiSeq Rapid Cluster Kit v2 (Illumina, Inc.) and HiSeq Rapid SBS Kit v2 (Illumina, Inc.).

After the library sequences were de-multiplexed, the quality of each sample library was assessed with respect to the number of reads per sample, mean quality score, and FASTQC parameters (Andrews 2010). Reads were then processed using Trimmomatic/0.35 with the options PE, ILLUMINACLIP: TruSeq2-PE.fa:2:30:10 LEADING:3 TRAILING:3 SLIDINGWINDOW:4:15 MINLEN:60 to remove any remaining adapter sequence, low quality reads, low quality read ends, and sequences shorter than 60 bases in length (Bolger et al. 2014). Sequence quality was then reevaluated via FASTQC (Andrews 2010). All sequences that passed the trimming and quality control with both reads in a pair present were aligned to the *Rattus norvegicus* Rnor_6.0 genome from NCBI downloaded on 31 July 2015, using HiSat2/2.1.0 (Kim et al. 2015) and Bowtie2/2.2.9 (Langmead and Salzberg 2012). Raw gene counts were assigned using Samtools/1.8 (Li et al. 2009), Python/2.7.3 and HTSeq/0.6.1 (Simon et al. 2015). Using edge R, raw counts were converted to counts per million (CPM) and log-CPM and then normalized (R Core Team 2018). Finally, differentially expressed genes were calculated using limma (Law et al. 2016). Differentially expressed genes were those genes with a fold change greater than 1.5-fold between the controls and the COV-exposed rats and an adjusted P value less than 0.05.

Statistical analysis of findings

Results for BAL parameters of cytotoxicity (LDH release), inflammation, and oxidant generation were expressed as mean values ± standard error (Table 1, Figures 1–3). For BAL LDH, cell counts, and phagocyte oxidant generation, data were analyzed using SigmaPlot for Windows Version 14.0 (Systat Software, Inc.; Ekrath, Germany). An analysis of variance was performed between the two treatment groups at each time point. Significant differences among groups were determined using the Student–Newman–Keuls *post hoc* test. BAL cytokine analyses were computed with JMP version 13.2 (SAS Institute, Cary NC, USA) using a Student's t-test to determine significant differences between group. Two-way (Treatment by Time) analyses of variance were utilized to examine differences in gene expression. Relevant scomparisons were generated using Fishers LSD with the pooled variance estimates. All differences were considered significant at $p < 0.05$.

Results

Lung histopathology

Under the conditions of this study, no consistent exposure-related morphologic alterations were observed in the lungs of the COV-exposed rats. Histopathologic alterations noted in rats in the study represented common incidental findings and occurred in both the air and COV groups, including a few foci of vascular mineralization, alveolar histiocytosis,

resolving hemorrhage, and small foci of inflammation that appeared to represent prior resolving hemorrhage. The most frequent observation was alveolar histiocytosis, an accumulation of alveolar macrophages. However, a limited number of foci of alveolar macrophages is expected in normal rats. In the 1-d post-exposure group, foci of alveolar histiocytosis were observed in 0/8 unexposed and 2/8 COV-exposed rats. In the 28 d post-exposure group, foci of alveolar histiocytosis were observed in 8/8 unexposed and 4/8 COV-exposed rats. In the 90 d post-exposure group, foci of alveolar histiocytosis were observed in 7/8 unexposed and 4/8 COV–exposed rats. Two rats (one control and one exposed) had foci of resolving pulmonary hemorrhage, which is an incidental finding in the lungs of rats. Three rats (two controls and one exposed), each had a small focus of histiocytic and neutrophilic inflammation that did not correlate with exposure and may have represented a late sequela to prior pulmonary hemorrhage. A slight increase in the number of alveolar macrophages and foci of accumulation can be an adaptive response to a need for increased phagocytosis and may be considered non-adverse in some toxicologic pathology studies (Nikula et al. 2014). For this study, a notation of focal alveolar histiocytosis was made when more than three alveolar macrophages were noted in an alveolus and/or multiple alveolar macrophages were seen in each of four or more adjacent alveoli and should not be interpreted as an adverse response. Foci with infiltrates of neutrophils accompanying macrophages were noted and scored separately. In this study, foci of alveolar histiocytosis never exceeded the normal range anticipated and increased with age, as is expected (Nikula et al. 2014). Based on the observed minimal to no differences observed in rats following sub-chronic exposure, tissues from the acute exposure were not evaluated.

Analysis of BALF LDH and cytokines

There were no significant differences in BALF LDH, a common measure of cytotoxicity, between the control and treatment groups in either the acute or sub-chronic exposure (Figure 1(A,B), respectively). A battery of proteins in BALF indicative of inflammation, immune function, and endothelial function were measured following the sub-chronic exposure to air or COV. At 1 d post-exposure to COV there were significant increases in leptin, IL-1β, IL-10, IP-10, and LIX, and at 28 d post-exposure VEGF was significantly increased (Table 1). Interestingly, at 90 d post-exposure, COV exposure caused decreases in GM-CSF, IFN-γ, GRO/KC, and VEGF when compared to the corresponding air group. No other significant differences were observed for any of the cytokines measured, at any timepoint (Table 1). Overall, the majority of cytokines in the panel were not altered, suggesting little overall effect of COV on lung inflammation and lung injury.

BAL cell counts and oxidant production by AMs

BAL cells were counted and differentiated following the acute and sub-chronic exposures at all time points. For both exposures, there were no significant differences in the total cells (Figure 2(A,B)), AMs/monocytes (Figure 2(C,D)), or neutrophils (Figure 2(E,F)) at any of the time intervals analyzed. For both exposures, at all time points >99% of the BAL cells were AM. There was an increase in the number of the neutrophils at 90 d post-exposure in the COV group *vs.* air following the sub-chronic exposure; however, the difference was not statistically significant. Eosinophils were largely not detected in either controls or exposed rats after sub-chronic exposure.

Oxidant production by AM in response to a stimulant (zymosan) was measured in AM recovered by BAL following both the acute and sub-chronic exposures (Figure 3(A,B), respectively). A significant increase was observed in the COV group at 1 d post-exposure following the acute exposure when compared to the Air group (Figure 3(A)). There was, however, no significant difference in this parameter following the sub-chronic exposure at any of the time intervals analyzed (Figure 3(B)).

Lung gene expression profile

No statistically significant changes in the global gene expression profiles were detected in the lungs of the acute COV-exposed animals at 1 d post-exposure. Statistically significant differential expression of forty-seven genes was detected in the acute COV exposed rat lungs at 28 d post-exposure (Table 2). The expressions of all forty-seven significantly differentially expressed genes (SDEGs) were down-regulated in the COV exposed rat lungs compared to those of the corresponding controls. In the acute COV exposed animal lungs, the gene *LOC102557529* exhibited the most significant differential expression, with a change in expression of −5.34-fold, compared with the air controls. Similar to the acute exposure group, significant gene expression changes were detected only at the 28 d post-exposure time interval in the rats in the sub-chronic COV exposure group (Table 2). All fifty-two SDEGs detected in this group, similar to the acute exposure group, were down-regulated compared with the corresponding control group. The most significant change in expression (−4.94-fold) was noticed in the case of the *Rsad2* gene. Thirty of the SDEGs detected in the COV exposed rats were found to be in common for the acute and sub-chronic exposures (Table 2).

Discussion

A series of studies have been conducted to understand the pulmonary and systemic effects of respiratory exposure to COV (Fedan et al. 2022; Krajnak et al. 2022; Sriram et al. 2022; and Weatherly et al. 2022). The goal of the current study was to evaluate the potential pulmonary toxicity of inhaled COV. In this study, whole-body, acute inhalation exposure (6 h) or a 28 d sub-chronic exposure (6 h/d × 4 d/wk × 4 wk) to 300 ppm COV did not cause changes in BAL inflammatory cells or cytotoxicity at either exposure duration. Also, no notable pulmonary pathology was observed following sub-chronic exposure. Changes in oxidant production by macrophages and lavage fluid cytokines related to inflammation, immune response and lung endothelial factors were minimal. Five of the 27 cytokines examined following sub-chronic exposure were increased at 1 d post-exposure; however, this did not persist at later time points. Interestingly, at 90 d post-exposure there were 4 cytokines that were significantly reduced (GM-CSF, IFN-γ, GRO/KC, and VEGF-A). Lung gene expression was performed and a down-regulation in gene expression was observed following both acute and sub-chronic exposure to COV at 28 d (47 genes in the acute exposure and 52 in the sub-chronic exposure). Although 30 of the genes were common to both exposure durations, they did not differ in degree of down-regulation between COV exposure durations.

The crude oil used in this study was Macondo surrogate oil mined in the Gulf of Mexico. Hydrocarbon analysis performed on this oil is presented in McKinney et al. (2022). The majority of hydrocarbons were in the aliphatic/paraffin group composed of a number of alkanes and isoalkanes with the most abundant being octane, heptane, hexane, nonane. These were followed in abundance by a number of higher alkanes, iso-alkane C5, 2- and 3-methylpentane, and 2- and 3- methylhexane. The most abundant compound overall was the cycloalkane methylcyclohexane. Also measured in this group were cyclohexane and methylcyclopentane. BTEX comprised the majority of the aromatic hydrocarbons with toluene and xylenes being in the greatest abundance, and propylbenzene and phenanthrene were also detected. In the exposure chamber (McKinney et al. 2022), BTEX (6.9, 14.7, 2.0, and 12.9 ppm, respectively) accounted for approximately 12% of the total VOC (~300 ppm) (McKinney et al. 2022). It should be noted that surrogate crude oil employed in this investigation is not representative of all crude oils, as their compositions are related to their geographical sites of origin, and this would affect the worker's exposure to VOCs.

There are relatively few studies that examined the average VOC exposure in upstream oil workers and in clean-up worker exposures. Several of these studies have been reviewed (Fedan et al. 2022; Fedan 2023) in this study series. In terms of up-stream exposures, exposure exceeding 100,000 ppm was measured and in incidents that resulted in worker death (NIOSH 2015; Retzer et al. 2018). In more routine activities upstream, short-term spikes of 2000 ppm are measured, and sustained levels can be as high as 500 ppm (Esswein et al. 2014a, 2014b). Relative to this type of exposure, a concentration of 300 ppm would be considered average to low depending on the operation. Oil spill exposure to VOC from vapors emitted from oil itself is more difficult to assess due to the numerous compounding factors in epidemiological studies including exposure to burning of oil in the spill. NIOSH conducted health hazard evaluations during the Deepwater Horizon oil spill (NIOSH 2011). In the operations where the personal breathing zone was monitored, exposure did not exceed occupational exposure limits for VOCs. Studies have been published related to data collected during the Gulf Long-term Follow-up study (Gulf Study) conducted by the National Institute for Environmental Health Science (Huynh et al. 2022) and with data released by British Petroleum (Avens et al. 2011) in regard to volatile levels workers may have experienced in clean-up of the Deepwater Horizon spill. These levels were much lower than those used in the current study, suggesting this exposure is on the higher end of what would be experienced in oil-spill clean-up operations from the oil slick alone. As mentioned above, different levels of VOCs emitted from oil spills will vary based on oil source and any extraction processes that may have occurred ahead of the spill make it difficult to assess how the concentration in this *in vivo* study would compare to that in clean-up operations outside of the burning operations.

As stated earlier, there is a significant body of *in vivo* research on exposures to fuel oils with high levels of VOCs; however, for comparative purposes to this study, there is a limited number of studies where exposure to crude oil or exposure scenarios mimic an oil spill (Fedan et al. 2022). In an associated Weatherly et al. (2022) analyzed BAL lymphocyte populations and observed increased subpopulations of lymphocytes at day 1 following acute exposure only; however, overall, lymphocytes accounted for less than 1% of the BAL cell population. However, lymphocytes and lymphocyte populations did not differ significantly

between air control and COV groups at any time following sub-chronic exposure (Weatherly et al. 2022).

In the current study, very little toxicity was observed in the lung in terms of pathology and lavage parameters related to inflammation and phagocyte oxidant production that can lead to oxidative stress typically associated with VOC exposure

A recent study by Amor-Carro et al. (2020), was designed to model an oil spill exposure related to the oil carried on the *Prestige*. Although this was a residual fuel oil (heavy fuel oil), the study design was similar to the present study in terms of VOC evaluation and endpoints measured (lung function, pulmonary pathology and lung lavage). Wistar and Brown Norway rats and C57BL6 mice were exposed in a nose-only chamber to the VOC generated from the oil for 2 hr/d, 5 d/wk for 3 wk. BTEX was measured in the chamber. The values were significantly lower than in the present study which may be expected from a residual fuel oil where refining to remove the lighter fraction of oil has occurred (Speight, 2014). No effects were observed in mice. Similar to the present study, there was a lack of evidence of inflammation in lung lavage parameters; however, despite this, rats showed decreased lung function and pulmonary pathology including peripheral (subpleural) emphysema. In addition, alveolar apoptosis and microvascular endothelial damage were observed. This finding differed markedly from the present study where there was no notable exposure-related pathology despite a higher concentration of BTEX. Reasons for the differences observed, other than oil source, may include assessment of emphysema in lungs from rats tracheotomized and used for pulmonary function testing and subsequently lavaged with 25 ml of saline in 5 ml fractions prior to fixation for histopathology and quantitative morphometry in the Amor-Carro study, with the potential to alter alveolar septal morphology. Additional differences included use of quantitative morphology methods for measuring emphysema in the Amor-Carro study. Other study differences included the use of different strains of rats, where the strains in the study by Amor-Carro et al. (Wistar and Brown-Norway) may be more sensitive to the exposure than Sprague-Dawley rats, and delivery method and effective dose. Amor-Carro et al. (2020) exposed the rats by nose-only exposure vs. the whole-body exposure in the current study. Nose-only exposure would have avoided exposure of the skin and more direct deposition of the aerosol in the lungs.

Unlike the present study, Amor-Carro et al. (2020), did not perform transcriptomics or assess gene expression in the lung. In general, there is very little information on gene expression following respiratory exposure to crude oil *in vivo*. In a study by Liu et al. (2020), mice were exposed by repeated oropharyngeal aspiration to a saline accommodated fraction of Macondo Well crude oil, COREXIT® dispersants, or a combination of oil and COREXIT®. The oil used in this study was from the same Macondo well as the present study. Lung RNA analysis and transcriptomics of the oil-exposed mice showed up-regulation of inflammatory pathways, including cytokine-cytokine receptor interaction and IL-17 and TNF-*a* signaling pathways. This study differed significantly from the current study as the whole crude oil was diluted and delivered directly to the lung via oropharyngeal aspiration, whereas in the present study, rats were exposed via whole-body inhalation to COV generated from surrogate crude oil.

In the present study, despite not detecting any morphologic, inflammatory, or cytotoxic changes in the lungs of rats exposed to COV, gene expression changes, albeit minimal, were detected in the same lung samples when global gene expression profiles were determined by NGS. The results obtained from the previous studies conducted in our laboratory have revealed significant changes, both with respect to the number of SDEGs detected and their fold changes in expressions, in response to inhalation exposure to aerosols containing toxic doses of particles such as crystalline silica (Sellamuthu et al. 2013), crystalline silica plus tobacco smoke (Sager et al. 2020), or nanocrystalline cellulose (Joseph et al. 2021). Unlike our previous studies (Sellamuthu et al. 2013; Sager et al. 2020; Joseph et al. 2021), in which significant differential expressions of hundreds or even thousands of genes were detected, only a limited number of genes (47 and 51 SDEGs in the acute and sub-chronic study, respectively) were found significantly differentially expressed in the lungs of the rats in response to their inhalation exposure to COV. Further, these changes were only observed at 28 d post-exposure. Similarly, the fold changes in the expressions of the SDEGs were several magnitudes lower in the COV exposed rat lungs (Table 2), compared to those observed under conditions that resulted in lung toxicity as reported in our previous studies (Sellamuthu et al. 2013; Sager et al. 2020; Joseph et al. 2021).

The changes in the lung gene expression profile detected, even though marginal, in the absence of any detectable lung toxicity in the oil vapor exposed rat lungs are likely due to the increased sensitivity of the transcriptome to respond to exposure to toxic materials compared to histological and biochemical endpoints of target organ toxicity (Hamadeh et al. 2002; Heinloth et al. 2004). However, the lack of duration-dependent changes in the expressions of the 30 SDEGs that are commonly detected in the acute and subchronic exposure conditions (Table 2) limit the interpretation of differentially expressed genes in the lung response to COV exposure. This is further strengthened by the finding that the expressions of many of the cytochrome P450 transcripts, known molecular targets for constituents of the VOCs (Sheets et al. 2004; Mendoza-Cantu et al. 2006; Zhao et al. 2007; James et al. 2008; Saint-Georges et al. 2008; Thomas et al. 2014) that were present in abundance in the COV, were unaffected in the rat lungs (data not presented). Since the minimal changes in the transcriptome detected in the COV exposed lungs were unlikely of any biological consequence, further studies investigating changes in the encoded proteins or pathway analysis of the SDEGs were not presently conducted.

Despite this finding, the presence of shared transcriptome changes in day 28 recovery groups, along with the suppression of select cytokines at day 28, remains a concern and suggests the need for follow-up study that evaluates a longer exposure period as well as longer recovery periods. As reviewed in Fedan (2023), BTEX exposure have been shown to lead to the development of various cancers, including blood, kidney, lung, and liver, as well as non-cancerous toxicity in these organ systems as well. The changes in the lung in regard to this exposure concentration and these durations appear to be somewhat minimal; however, the assessment of the development of some of the chronic diseases associated with BTEX exposures, including cancers, would require observation over a much longer latency period

In summary, this study was designed to mimic exposure in the upstream oil industry and exposure that may occur in oil-spill clean-up operations. Relatively little pulmonary

toxicity was observed in terms of lung injury and inflammation. This combined with the gene expression data, suggests minimal effects in lung response to whole-body inhalation exposure to COV in the rats under the exposure conditions employed in this study. The study was designed to mimic a lower exposure concentration scenario in the industry; however, it is important to note some important aspects in the exposure paradigm. The study did not examine a dose-response, but instead evaluated a single concentration at two different exposure durations. Even though the generated concentration inside of the COV exposure chambers was 300 ppm, the deposited lung dose in the rats is not known. With a whole-body inhalation exposure during the light cycle, animal activity is typically low during the exposure timeframe, whereas a worker would be active during exposure and, hence, have a higher rate of respiration leading to higher deposited dose in the lung. Low activity level combined with the general instability of VOCs likely led to a lower deposited dose from exposure than an oil worker may typically experience during a workday. This fact may help explain the lack of overt toxicity data in our current animal study.

Funding

Funding was provided by the National Institute for Occupational Safety and Health, Project Number 7927ZLDC.

Data availability statement

The Next Generation Sequence data discussed in this publication have been deposited in NCBI's Gene Expression Omnibus (GEO) and are accessible through GEO Series accession number GSE152187.

References

Alexander M, Engel LS, Olaiya N, Wang L, Barrett J, Weems L, Schwartz EG, Rusiecki JS. 2018. The Deepwater Horizon oil spill coast guard cohort study: a cross-sectional study of acute respiratory health symptoms. Environ Res. 162:196–202. doi: 10.1016/j.envres.2017.11.044. [PubMed: 29331799]

Amor-Carro Ó, White KM, Fraga-Iriso R, Mariñas-Pardo LA, Núñez-Naveira L, Lema-Costa B, Villarnovo M, Verea-Hernando H, Ramos-Barbón D. 2020. Airway hyperresponsiveness, inflammation, and pulmonary emphysema in rodent models designed to mimic exposure to fuel oil-derived volatile organic compounds encountered during an experimental oil spill. Environ Health Perspect. 128(2):27003–27014. doi: 10.1289/EHP4178. [PubMed: 32074461]

Andrews S 2010. FastQC: a quality control tool for high throughput sequence data. http://www.bioinformatics.babraham.ac.uk/projects/fastqc.

Antonini JM, Van Dyke K, Ye Z, DiMatteo M, Reasor MJ. 1994. Introduction of luminal-dependent chemiluminescence as a method to study silica inflammation in the tissue and phagocytic cells of rat lung. Environ Health Perspect. 102:37–42.

ATSDR. 1995. Toxicological profile for polycyclic aromatic hydrocarbons (PAHs). Atlanta, GA: U.S. Department of Health and Human Services. https://wwwn.cdc.gov/TSP/ToxProfiles/ToxProfiles.aspx?id=122&tid=25.

ATSDR. 1999a. Toxicological profile for n-hexane. Atlanta, GA: U.S. Department of Health and Human Services. https://www.atsdr.cdc.gov/ToxProfiles/tp113.pdf.

ATSDR. 1999b. Toxicological profile for total petroleum hydrocarbons. Atlanta, GA: U.S. Department of Health and Human Services. https://wwwn.cdc.gov/TSP/ToxProfiles/ToxProfiles.aspx?id=424&tid=75.

ATSDR. 2004. Interaction profile for benzene, toluene, ethylbenzene, and xylenes (BTEX). Atlanta, GA: U.S. Department of Health and Human Services. K:\DTFiles\Tox Info Branch\Toxicological Profiles Documents\Interaction Profiles\IP for BTEX\Final\BTEX.Finalmay04.wpd (cdc.gov).

ATSDR. 2005. Toxicological profile for naphthalene, 1-methylnaphthalene, and 2-methylnaphthalene. Atlanta, GA: U.S. Department of Health and Human Services. https://wwwn.cdc.gov/TSP/ToxProfiles/ToxProfiles.aspx?id=240&tid=43.

ATSDR. 2007a. Toxicological profile for benzene. Atlanta, GA: U.S. Department of Health and Human Services. https://wwwn.cdc.gov/TSP/ToxProfiles/ToxProfiles.aspx?id=40&tid=14.

ATSDR. 2007b. Toxicological profile for xylene. Atlanta, GA: U.S. Department of Health and Human Services. https://wwwn.cdc.gov/TSP/ToxProfiles/ToxProfiles.aspx?id=296&tid=53.

ATSDR. 2010. Toxicological profile for ethylbenzene. Atlanta, GA: U.S. Department of Health and Human Services. https://wwwn.cdc.gov/TSP/ToxProfiles/ToxProfiles.aspx?id=383&tid=66.

ATSDR. 2017. Toxicological profile for toluene. Atlanta, GA: U.S. Department of Health and Human Services. https://wwwn.cdc.gov/TSP/ToxProfiles/ToxProfiles.aspx?id=161&tid=29.

Avens HJ, Unice KM, Sahmel J, Gross SS, Keenan JJ, Paustenbach DJ. 2011. Analysis and modeling of airborne BTEX concentrations from the Deepwater Horizon oil spill. Environ Sci Technol. 45(17):7372–7379. doi: 10.1021/es200963x. [PubMed: 21797246]

Bolger AM, Lohse M, Usadel B. 2014. Trimmomatic: a flexible trimmer for Illumina sequence data. Bioinformatics. 30(15):2114–2120. doi: 10.1093/bioinformatics/btu170. [PubMed: 24695404]

Carrillo J-C, David Adenuga M, McKee RH, Roth RN, Steup D, Simpson BJ. 2013. The sub-chronic toxicity in rats of isoparaffinic solvents. Reg Toxicol Pharmacol. 67(3):446–455. doi: 10.1016/j.yrtph.2013.09.004.

Castranova V, Jones T, Barger M, Afshari A, Frazer DJ. 1990. Pulmonary responses of guinea pigs to consecutive exposures to cotton dust. In: Jacobs RR, Wakelyn PJ, Domelsmith LN, editors. Proceedings of the 14th Cotton Dust Research Conference. Memphis, TN: National Cotton Council; p. 131–135.

Chen WH, Chen ZB, Yuan CS, Hung CH, Ning SK. 2016. Investigating the differences between receptor and dispersion modeling for concentration prediction and health risk assessment of volatile organic compounds from petrochemical industrial complexes. J Environ Manag. 166:440–449. doi: 10.1016/j.jenvman.2015.10.050.

D'Andrea MA, Reddy GK. 2014. Crude oil spill exposure and human health risks. J Environ Occup Med. 56(10):1029–1041. doi: 10.1097/JOM.0000000000000217.

D'Andrea MA, Reddy GK. 2018. The development of long-term adverse health effects in oil spill cleanup workers of the Deepwater Horizon offshore drilling rig disaster. Front Public Health. 6:1–8. doi: 10.3389/fpubh.2018.00117. [PubMed: 29404319]

Divine BJ, Hartman CM. 2000. Update of a study of crude oil petroleum workers 1946–94. Occup Environ Med. 57(6):411–417. doi: 10.1136/oem.57.6.411. [PubMed: 10810131]

Divine BJ, Barron V. 1987. Texaco mortality study: III. A cohort study of producing and pipeline workers. Am J Ind Med. 11(2):189–202. doi: 10.1002/ajim.4700110208. [PubMed: 3826079]

Esswein EJ, Snawder J, King B, Breitenstein M, Alexander-Scott M, Kiefer M. 2014a. Evaluation of some potential chemical exposure risks during flowback operations in unconventional oil and gas extraction: preliminary results. J Occup Environ Hyg. 11(10):D174–D184. doi: 10.1080/15459624.2014.933960. [PubMed: 25175286]

Esswein EJ, Snawder J, King B, Breitenstein M, Alexander-Scott M. 2014b. Preliminary field studies on worker exposures to volatile chemicals during oil and gas extraction flowback and production testing operations. https://blogs.cdc.gov/niosh-science-blog/2014/08/21/flowback-2/.

Fedan JS. 2023. Biological effects of inhaled crude oil vapor. Toxicology (Submitted).

Fedan JS, Thompson JA, Russ KA, Dey RD, Reynolds JS, Kashon ML, Jackson MC, McKinney W. 2022. Biological effects of inhaled crude oil vapor. II. Pulmonary effects. Toxicol Appl Pharmacol. 1450:116154. doi: 10.1016/j.taap.2022.116154.

Fischäder G, Röder-Stolinski C, Wichmann G, Nieber K, Lehmann I. 2008. Release of MCP-1 and IL-8 from lung epithelial cells exposed to volatile organic compounds. Toxicol in Vitro. 22(2):359–366. doi: 10.1016/j.tiv.2007.09.015. [PubMed: 17993253]

Hamadeh H, Bushel P, Jayadev S, DiSorbo O, Bennett L, Li L, Tennant R, Stoll R, Barrett J, Paules R, et al. 2002. Prediction of compound signature using high density gene expression profiling. Toxicol Sci. 67(2):232–240. [PubMed: 12011482]

Harrison RJ, Retzer K, Kosnett MJ, Hodgson M, Jordan T, Ridl S, Kiefer M. 2016. Sudden deaths among oil and gas extraction workers resulting from oxygen deficiency and inhalation of hydrocarbon gases and vapors – United States, January 2010 – March 2015. MMWR Morb Mortal Wkly Rep. 65(1):6–9., doi: 10.15585/mmwr.mm6501a2. [PubMed: 26766558]

Hawley GG. 1981. The condensed chemical dictionary. 10th ed. New York, Van Nostr and Reinhold; p. 792.

Heinloth AN, Irwin RD, Boorman GA, Nettesheim P, Fannin RD, Sieber SO, Snell ML, Tucker CJ, Li L, Travlos GS, et al. 2004. Gene expression profiling of rat livers reveals indicators of potential adverse effects. Toxicol Sci. 80(1):193–202. doi: 10.1093/toxsci/kfh145. [PubMed: 15084756]

Hubbs AF, Castranova V, Ma JCY, Frazer DG, Siegel PD, Ducatman BS, Grote A, Schwegler-Berry D, Robinson VA, Van Dyke C, et al. 1997. Acute lung injury induced by a commercial leather conditioner. Toxicol Appl Pharmacol. 143(1):37–46. doi: 10.1006/taap.1996.8053. [PubMed: 9073590]

Huynh TB, Groth CP, Ramachandran G, Banerjee S, Stenzel M, Blair A, Sandler DP, Engel LS, Kwok RK, Stewart PA. 2022. Estimates of inhalation exposures to oil-related components on the supporting vessels during the Deepwater Horizon oil spill. Ann Work Expo Health. 66(Suppl 1):i111–i123. doi: 10.1093/annweh/wxaa113. [PubMed: 33791771]

IARC. 1989. IARC monographs on the evaluation of carcinogenic risk to humans: occupational exposures in petroleum refining: crude oil and major petroleum fuels. Lyon: IARC; p. 1–321.

James CA, Xin G, Doty SL, Strand SE. 2008. Degradation of low molecular weight volatile organic compounds by plants genetically modified with mammalian cytochrome P450 2E1. Environ Sci Technol. 42(1):289–293. doi: 10.1021/es071197z. [PubMed: 18350910]

Jordan T 2015. Hydrocarbon exposures during tank gauging and sampling operations. www.stepsnetwork.com/member-presentations/file/Tank_GaugingMonitoring_Results%252Epdf.

Joseph P, Umbright CM, Roberts JR, Cumpston JL, Orandle MS, McKinney WG, Sager TM. 2021. Lung toxicity and gene expression changes in response to whole-body inhalation exposure to cellulose nanocrystal in rats. Inhal Toxicol. 33(2):66–80. doi: 10.1080/08958378.2021.1884320. [PubMed: 33602020]

Khalil C, Nasir J. 2010. Toxicity of volatile organic compounds (VOCs) mixtures using human derived cells. WIT Trans Environ. 132:3–12.

Kim D, Langmead B, Salzberg SL. 2015. HISAT: a fast spliced aligner with low memory requirements. Nat Methods. 12(4):357–360. doi: 10.1038/nmeth.3317. [PubMed: 25751142]

Krajnak K, Russ KA, McKinney W, Waugh S, Zheng W, Kan W, Kashon ML, Cumpston J, Fedan JS. 2022. Biological effects of inhaled vapors from crude oil. IV. Cardiovascular effects. Toxicol Appl Pharmacol. 15447:116071. doi: 10.1016/j.taap.2022.116071.

Kwok RK, Engel LS, Miller AK, Blair A, Curry MD, Jackson WB II, Stewart PA, Stenzel MR, Birnbaum LS, Sandler DP, Gulf Study Research Team. 2017. The Gulf study. A prospective study of persons involved in the Deepwater Horizon oil spill response and clean-up. Environ Health Perspect. 125(4):570–578. doi: 10.1289/EHP715. [PubMed: 28362265]

Langmead B, Salzberg SL. 2012. Fast gapped-read alignment with Bowtie 2. Nat Methods. 9(4):357–359. doi: 10.1038/nmeth.1923. [PubMed: 22388286]

Law CW, Alhamdoosh M, Su S, Dong X, Tian L, Smyth GK, Ritchie ME. 2016. RNA-seq analysis is easy as 1–2-3 with limma, Glimma and edgeR. F1000Res. 5:1408. doi: 10.12688/f1000research.9005.2.

Li H, Handsaker B, Wysoker A, Fennell T, Ruan J, Homer N, Marth G, Abecasis G, Durbin R, 1000 Genome Project Data Processing Subgroup. 2009. 1000 Genome project data processing subgroup 2009. The sequence alignment/map format and SAMtools. Bioinformatics. 25(16):2078–2079. doi: 10.1093/bioinformatics/btp352. [PubMed: 19505943]

Lin CY, Tjeerdema RS. 2008. Crude oil, oil, gasoline and petrol. In: Jorgensen SE and Fath BD (Eds.). Encyclopedia of ecology. Amsterdam, Netherlands: Elsevier, Inc.; p. 797–805.

Liu YZ, Miller CA, Zhuang Y, Mukhopadhyay SS, Saito S, Overton EB, Morris GF. 2020. The impact of the Deepwater Horizon oil spill upon lung health – mouse model-based RNA-Seq analysis. IJERPH. 17(15):5466. doi: 10.3390/ijerph17155466. [PubMed: 32751227]

Mckee RH, Adenuga MD, Carrillo J-C. 2015. Characterization of the toxicological hazards of hydrocarbon solvents. Crit Rev Toxicol. 45(4):273–365. doi: 10.3109/10408444.2015.1016216. [PubMed: 25868376]

McKinney W, Jackson MC, Law B, Fedan J. 2022. Automated crude oil vapor inhalation exposure system. Inhal Toxicol. 34(11–12):340–349. doi: 10.1080/08958378.2022.2114562. [PubMed: 36007004]

Mendoza-Cantú A, Castorena-Torres F, Bermúdez de León M, Cisneros B, López-Carrillo L, Rojas-Garc ıa AE, Aguilar-Salinas A, Manno M, Albores A. 2006. Occupational toluene exposure induces cytochrome P450 2E1 mRNA expression in peripheral lymphocytes. Environ Health Perspect. 114(4):494–499. doi: 10.1289/ehp.8192. [PubMed: 16581535]

Nikula K, McCartney J, McGovern T, Miller G, Odin M, Pino V, Reed M. 2014. STP position: interpreting the significance of increased alveolar macrophages in rodents following inhalation of pharmaceutical materials. Toxicol Pathol. 42(3):472–486. doi: 10.1177/0192623313507003. [PubMed: 24178583]

NIOSH. 2015. Suspected inhalation fatalities involving workers during manual tank gauging, sampling, and fluid transfer operations on oil and gas well sites, 2010–2014. Cincinnati, OH: U.S. Department of Health and Human Services, Centers for Disease Control and Prevention, National Institute for Occupational Safety and Health, http://www.cdc.gov/niosh/topics/fog/data.html.

NIOSH. 2011. Health hazard evaluation of Deepwater Horizon response workers [pdf]. HETA 2010–0115 & 2010–0129–3138. [accessed 2022 Jul 7] https://www.cdc.gov/niosh/hhe/reports/pdfs/2010-0115-0129-3138.pdf.

R Core Team. 2018. R: a language and environment for statistical computing. Vienna, Austria: R Foundation for Statistical Computing.

Retzer K, Schmick E, Ramirez-Cardenas A, King B, Snawder J. 2018. Gases and vapors continue to pose hazards on oil and gas well sites during gauging, fluid transfer, and disposal. https://blogs.cdc.gov/niosh-science-blog/2018/08/24/oil-and-gas-vapors/.

Sager TM, Umbright CM, Mustafa GM, Yanamala N, Leonard HD, McKinney WG, Kashon ML, Joseph P. 2020. Tobacco smoke exposure exacerbated crystalline silica-induced lung toxicity in rats. Toxicol Sci. 178(2):375–390. doi: 10.1093/toxsci/kfaa146. [PubMed: 32976597]

Saint-Georges F, Abbas I, Billet S, Verdin A, Gosset P, Mulliez P, Shirali P, Garçon G. 2008. Gene expression induction of volatile organic compound and/or polycyclic aromatic hydrocarbon-metabolizing enzymes in isolated human alveolar macrophages in response to airborne particulate matter (PM2.5). Toxicology. 244(2–3):220–230. doi: 10.1016/j.tox.2007.11.016. [PubMed: 18178302]

Sathiakumar NE, Delzell E, Cole P, Brill I, Frisch J, Spivey G. 1995. A case control study of leukemia among petroleum workers. J Occ Environ Med. 37(11):1269–1277. doi: 10.1097/00043764-199511000-00005.

Schnatter AR, Theriault G, Katz AM, Thompson FS, Donaleski D, Murray N. 1992. A retrospective mortality study within operating segments of a petroleum company. Am J Ind Med. 22(2):209–229. doi: 10.1002/ajim.4700220207. [PubMed: 1415287]

Sellamuthu R, Umbright C, Roberts JR, Cumpston A, McKinney W, Chen BT, Frazer D, Li S, Kashon M, Joseph P. 2013. Molecular insights into the progression of crystalline silica-induced pulmonary toxicity in rats. J Appl Toxicol. 33(4):301–312. doi: 10.1002/jat.2733. [PubMed: 22431001]

Sellamuthu R, Umbright C, Roberts JR, Chapman R, Young SH, Richardson D, Leonard H, McKinney W, Chen B, Frazer D, et al. 2011. Blood gene expression profiling detects silica exposure and toxicity. Toxicol Sci. 122(2):253–264. doi: 10.1093/toxsci/kfr125. [PubMed: 21602193]

Sheets PL, Yost GS, Carlson GP. 2004. Benzene metabolism in human lung cell lines BEAS-2B and A549 and cells overexpressing CYP2F1. J Biochem Mol Toxicol. 18(2):92–99. doi: 10.1002/jbt.20010. [PubMed: 15122651]

Simon A, Pyl PT, Huber W. 2015. HTSeq—A Python framework to work with high-throughput sequencing data. Bioinformatics. 31(2): 166–169. doi: 10.1093/bioinformatics/btu638. [PubMed: 25260700]

Speight JG 2014. Residual fuel oil. In: Speight JG. editor. Handbook of petroleum product analysis. 2nd Edition. Hoboken, NJ: John Wiley and Sons, Inc.; p. 186–206.

Sriram K, Lin GX, Jefferson AM, McKinney W, Jackson MC, Cumpston JL, Cumpston JB, Leonard HD, Kashon ML, Fedan JS. 2022. Biological effects of inhaled crude oil vapor. V. Altered biogenic amine neurotransmitters and neural protein expression. Toxicol Appl Pharmacol. 449:116137. doi: 10.1016/j.taap.2022.116137. [PubMed: 35750205]

Stenehjem JS, Kjaerheim K, Rabanal KS, Grimsrud TK. 2014. Cancer incidence among 14000 offshore oil industry workers. Occ Med. 64(7):539–545. doi: 10.1093/occmed/kqu111.

Thomas R, Hubbard AE, McHale CM, Zhang L, Rappaport S, Lan Q, Rothman N, Vermeulen R, Guyton K, Jinot J, et al. 2014. Characterization of changes in gene expression and biochemical pathways at low levels of benzene exposure. PLOS One. 9(5):e91828. doi: 10.1371/journal.pone.0091828. [PubMed: 24786086]

U.S. Coast Guard. 2011. Final report. BP Deepwater Horizon oil spill incident specific preparedness review January 2011 [report]. https://homeport.uscg.mil/Lists/Content/Attachments/1040/DWH%20ISPR%202011.pdf.

Valentic D, Stojanovic D, Micovic V, Vukelic M. 2005. Work related diseases and injuries on an oil rig. Int Marit Health. 56:56–66. [PubMed: 16532585]

Verma DK, Johnson DM, McLean JD. 2000. Benzene and total hydrocarbon exposures in the upstream petroleum oil and gas industry. AIHAJ. 61(2):255–263. doi: 10.1202/0002-8894(2000)061<0255:BATHEI>2.0.CO;2. [PubMed: 10782197]

Wang F, Li C, Liu W, Jin Y, Guo L. 2014. Effects of subchronic exposure to low-dose volatile organic compounds on lung inflammation in mice. Environ Toxicol. 29(9):1089–1097. doi: 10.1002/tox.21844. [PubMed: 23418084]

Weatherly LM, Shane HL, Baur R, Lukomska E, Roberts JR, Fedan JS, Anderson SE. 2022. Biological effects of inhaled crude oil vapor. VI. Immunotoxicity. Toxicol Appl Pharmacol. 499:116100.

Wong O, Raabe GK. 2000. A critical review of cancer epidemiology in the petroleum industry, with a meta-analysis of a combined database of more than 350,000 workers. Reg Toxicol Pharmacol. 32(1):78–98. doi: 10.1006/rtph.2000.1410.

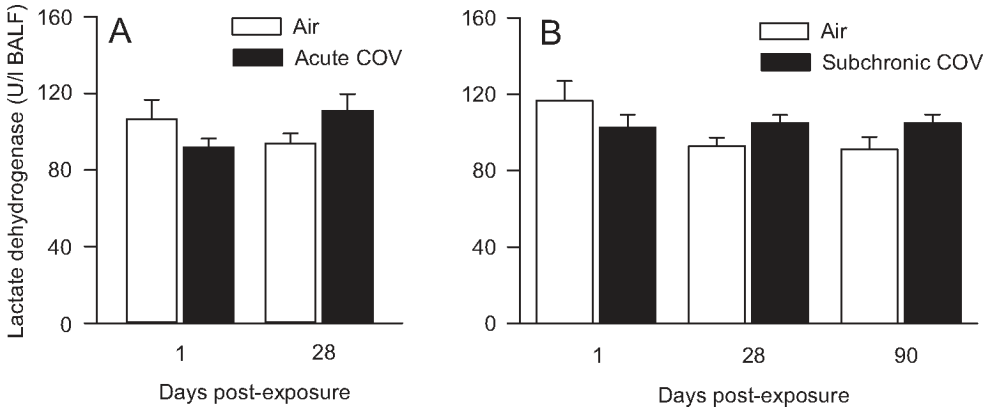

Figure 1.

Lactate dehydrogenase (LDH) activity in bronchoalveolar lavage fluid (BALF) recovered from rats at 1- and 28 d post-exposure to air or 300 ppm COV 6 hr/d for 1 day (A, acute COV) or at 1, 28, and 90 d after the last day of exposure to 300 ppm in the sub-chronic exposure of 6 hr/d for 4 d/wk for 4 wk (B, sub-chronic COV). No significant differences were observed between groups in either exposure. $n = 8$ per group per timepoint.

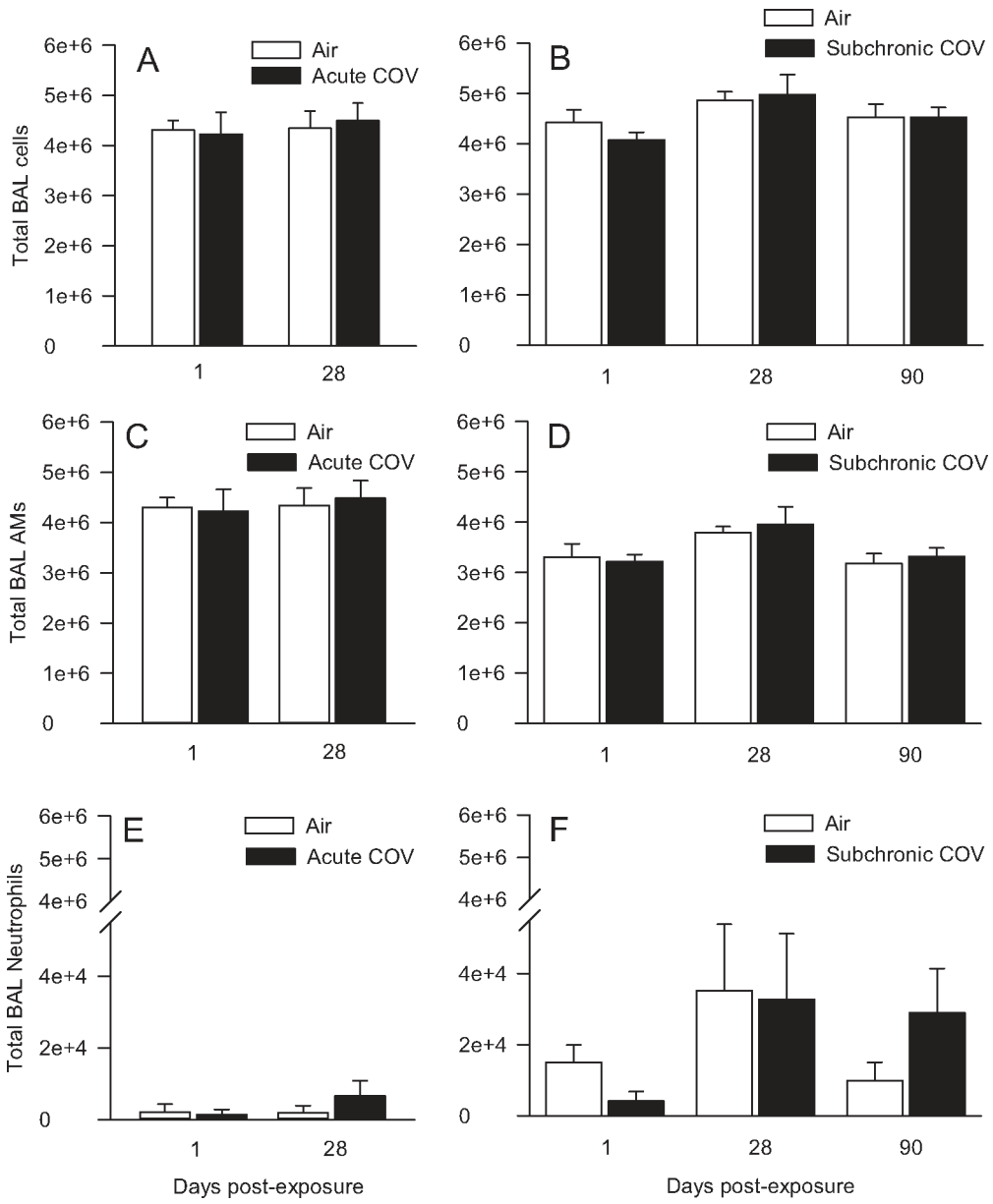

Figure 2.

Bronchoalveolar lavage (BAL) cells were recovered from rats and enumerated at 1 and 28 d post-exposure to air or 300 ppm COV 6 hr/d for 1 day (acute COV) or at 1, 28, and 90 days after the last day of exposure to 300 ppm for 6 hr/d for 4 d/wk for 4 wk (sub-chronic COV): total BAL cells recovered following acute (A) and sub-chronic (B) exposures, total alveolar macrophages (AM) following acute (C) and sub-chronic (D) exposure, and total neutrophils following acute (E) and sub-chronic (F) exposure. Lymphocyte and eosinophils not shown. AM accounted for >99% of all cells for all groups at all time points. No significant differences were observed. $n = 8$ per group per timepoint.

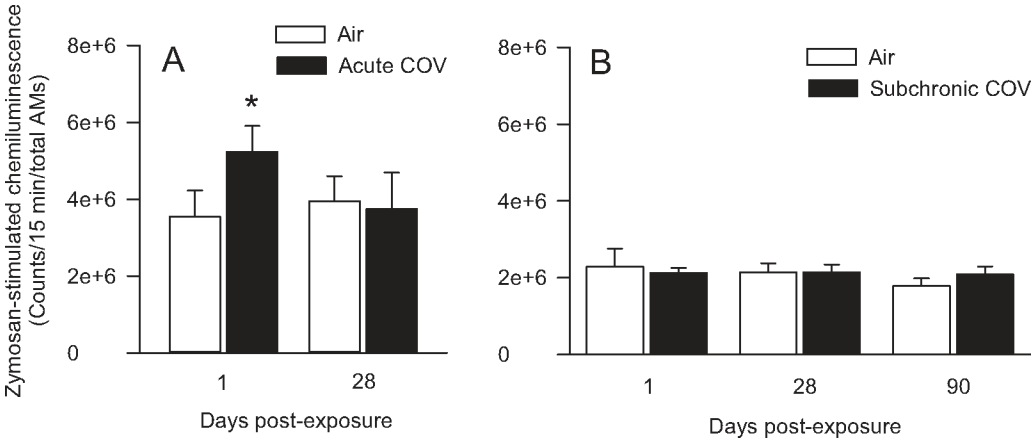

Figure 3.

Oxidant production by bronchoalveolar (BAL) alveolar macrophages (AM) recovered from rats at 1 and 28 d post-exposure to air or 300 ppm COV 6 hr/d for 1 day (A, acute COV) or at 1, 28, and 90 d after the last day of exposure to 300 ppm for 6 hr/d for 4 d/wk for 4 wk (B, sub-chronic COV) was measured by evaluating chemiluminescence in the presence of zymosan. *Significantly different from air, $p \leq 0.05$. $n = 8$ per group per timepoint.

Table 1.

BALF cytokines (pg/ml ±standard error) in rats at 1, 28, and 90days following the last day of the 4 wk sub-chronic exposure to Air or COV (300 ppm, 6 hr/d, 4 d/wk, 4 wk).

Cytokine	Air 1 d	COV 1 d	Air 28 d	COV 28 d	Air 90 d	COV 90 d
G-CSF	0.23 ± 0.16	0.16 ± 0.15	0.16 ± 0.15	0.16 ± 0.10	0.08 ± 0.08	0.08 ± 0.08
Eotaxin	1.53 ± 0.35	1.80 ± 0.40	2.00 ± 0.23	1.83 ± 0.34	2.00 ± 0.43	1.61 ± 0.38
GM-CSF	7.70 ± 1.51	13.1 ± 3.28	10.7 ± 1.84	14.3 ± 2.09	14.5 ± 1.30	8.35 ± 1.60 *
IL-1α	8.95 ± 1.25	10.2 ± 1.17	12.1 ± 1.36	13.0 ± 0.93	16.0 ± 1.36	12.9 ± 1.56
Leptin	9.42 ± 1.59	29.5 ± 6.01 *	18.7 ± 2.89	18.8 ± 2.76	19.1 ± 2.31	20.2 ± 2.60
MIP-1α	2.06 ± 0.26	2.63 ± 0.24	2.69 ± 0.30	2.31 ± 0.24	3.76 ± 0.44	3.84 ± 0.70
IL-4	5.51 ± 0.81	6.34 ± 1.42	8.64 ± 1.09	8.52 ± 1.27	8.20 ± 1.49	5.62 ± 0.99
IL-1β	13.2 ± 1.44	22.9 ± 3.45 *	14.5 ± 0.63	16.9 ± 1.78	21.1 ± 1.18	16.69 ± 1.54
IL-2	1.83 ± 1.27	6.15 ± 3.41	5.08 ± 1.51	9.62 ± 1.98	10.9 ± 1.92	6.59 ± 1.49
IL-6	227 ± 29.9	274 ± 41.3	263 ± 35.5	282 ± 58.6	343 ± 34.7	307 ± 13.8
EGF	1.70 ± 0.17	2.74 ± 0.79	1.92 ± 0.34	10.9 ± 8.04	1.78 ± 0.27	1.46 ± 0.15
IL-13	4.35 ± 0.55	4.87 ± 0.69	6.01 ± 0.84	5.63 ± 0.76	6.51 ± 0.49	6.43 ± 0.68
IL-10	4.77 ± 1.42	9.60 ± 1.92 *	7.91 ± 0.76	8.11 ± 1.58	8.69 ± 1.48	7.46 ± 0.60
IL-12p70	5.88 ± 2.25	2.02 ± 1.06	2.70 ± 1.21	5.49 ± 1.53	3.33 ± 1.23	6.61 ± 1.01
IFN-γ	3.74 ± 1.69	2.97 ± 1.38	1.67 ± 0.99	1.14 ± 0.29	21.0 ± 4.14	14.35 ± 2.18 *
IL-5	12.1 ± 1.58	10.6 ± 2.17	12.5 ± 1.56	13.6 ± 1.23	13.9 ± 1.24	12.7 ± 1.35
IL-17A	1.75 ± 0.17	2.37 ± 0.40	2.96 ± 0.29	3.31 ± 0.16	2.93 ± 0.23	2.16 ± 0.17
IL-18	293 ± 47.4	389 ± 64.2	249 ± 16.8	303 ± 24.1	464 ± 71.0	352 ± 47.0
MCP-1	101 ± 14.5	109 ± 16.6	67.2 ± 15.1	90.8 ± 16.5	92.0 ± 8.70	107 ± 11.7
IP-10	4.35 ± 0.62	7.01 ± 1.11 *	4.11 ± 1.10	2.65 ± 0.69	4.81 ± 0.90	4.54 ± 0.72
GRO/KC	43.6 ± 7.29	60.9 ± 8.46	66.4 ± 4.81	76.8 ± 11.4	115 ± 17.4	69.0 ± 5.06 *
VEGF-A	1240 ± 210	1110 ± 153	1950 ± 333	3220 ± 638 *	4170 ± 350	2540 ± 649 *
Fractalkine	43.9 ± 3.40	38.6 ± 2.43	52.9 ± 5.45	58.6 ± 9.32	71.3 ± 6.37	73.2 ± 5.91
LIX	3.98 ± 1.39	15.1 ± 3.66 *	9.18 ± 1.53	9.01 ± 2.58	21.1 ± 5.06	17.0 ± 6.13
MIP-2	22.1 ± 3.90	30.5 ± 5.58	34.0 ± 3.55	43.1 ± 6.60	50.3 ± 4.19	45.3 ± 4.10

Cytokine	Air 1 d	COV 1 d	Air 28 d	COV 28 d	Air 90 d	COV 90 d
TNFα	0.24 ± 0.04	0.43 ± 0.12	0.35 ± 0.09	0.36 ± 0.08	0.34 ± 0.09	0.37 ± 0.14
RANTES	0.78 ± 0.06	0.88 ± 0.11	0.64 ± 0.08	0.63 ± 0.04	0.71 ± 0.09	0.72 ± 0.06
IL-35	226 ± 110	193 ± 133	187 ± 24.2	183 ± 23.3	199 ± 29.2	193 ± 10.2
TGF-β	54.8 ± 2.59	65.5 ± 5.02	67.5 ± 5.44	72.7 ± 8.66	57.3 ± 5.51	69.2 ± 7.39

Note: Cytokine abbreviations are noted in the methods section. IL-27 and CCK were below the limit of detection for all samples (data not shown).

indicates significant difference between air and COV groups, $p \leq 0.05$.

Table 2.

Significantly differentially expressed genes detected in the rat lungs exposed to crude oil vapor.

Transcript	Fold change in expression Acute	Sub-chronic
Ankyrin repeat and BTB domain containing 1 (ABTB1)	−1.64	NS
Adiponectin receptor 1 (ADIPOR1)	NS	−1.67
Alpha hemoglobin stabilizing protein (AHSP)	−3.57	NS
5'-aminolevulinate synthase (ALAS2)	**−4.11**	**−4.75**
Arachidonate 15-lipoxygenase (ALOX15)	NS	−2.80
Rho guanine nucleotide exchange factor 37 (ARHGEF37)	−2.08	NS
ATPase inhibitory factor 1 (ATPIF1)	NS	−1.52
BCAS2, pre-mRNA processing factor (BCAS2)	**−1.81**	**−1.91**
BCL2 interacting protein 3 like (BNIP3L)	−1.75	NS
CD226 Molecule (CD226)	**−2.41**	**−2.31**
C-type lectin domain family 1, member B (CLEC1B)	**−3.85**	**−4.20**
C-x(9)-C motif containing (CMC2)	−1.62	NS
Cytidine/uridine monophosphate kinase 2 (CMPK2)	NS	−1.56
Cellular repressor of E1A-stimulated genes 1 (CREG1)	NS	−1.59
Death-associated protein kinase 2 (DAPK2)	NS	−1.53
E2F transcription factor 2 (E2F2)	**−1.81**	**−1.99**
Erythrocyte Membrane Protein Band 4.1 (EPB4.1)	NS	−1.55
Erythrocyte membrane protein band 4.2 (EPB4.2)	−2.60	NS
Ecotropic viral integration site 2 A (EVi2A)	**−1.70**	**−1.69**
Coagulation factor II (thrombin) receptor-like 2 (F2FL2)	**−2.76**	**−2.78**
Coagulation factor XIII A1 chain (F13A1)	**−2.21**	**−2.42**
Family with sequence similarity 46, member C (FAM46C)	**−3.12**	**−3.65**
Ferrochelatase (feCH)	**−2.15**	**−2.28**
GABA type A receptor associated protein like 2 (GABARAPL2)	NS	−2.02
Glutaredoxin 5 (GLRX5)	**−2.43**	**−2.84**
Glycoprotein VI (GP6)	NS	−2.70
Glycoprotein IX (GP9)	**−4.73**	**−2.87**
Glutathione peroxidase 1 (GPX1)	**−1.64**	**−1.66**

Transcript	Fold change Acute	in expression Sub-chronic
GRB2-related adaptor protein 2 (GRAP2)	NS	−1.89
Histone cluster 3, Hb2a (HIST3H2BA)	**−3.52**	**−3.12**
Interferon Induced Protein with Tetratricopeptide Repeats 1 (IFIT1LB)	NS	−1.96
Iron-sulfur cluster assembly 1 (ISCA1)	**−1.66**	**−1.90**
Integrin subunit alpha 2b (ITGA2B)	**−2.54**	**−2.65**
Potassium voltage-gated channel subfamily A member regulatory beta subunit 1 (KCNAB1)	NS	−3.11
Tumor protein, translationally-controlled 1 (LOC100360791)	NS	−1.55
Uncharacterized LOC100910650 (LOC100910650)	NS	−3.50
Uncharacterized LOC102557529 (LOC102557529)	−5.34	NS
Uncharacterized LOC102550818 (LOC102550818)	**−3.62**	**−3.61**
RNA, 7SL, cytoplasmic 1(LOC102723236)	NS	−1.68
Lymphocyte antigen 6 family member G6F (LY6G6F)	**−5.05**	**−3.68**
Membrane associated ring-CH-type finger 2 (MARCH2)	**−1.85**	**−1.99**
Makorin ring finger protein 1 (MKRN 1)	**−1.58**	**−1.68**
Nuclear receptor coactivator 4 (NCOA4)	**−2.18**	**−2.47**
Nuclear factor, erythroid 2 (NFE2)	**−1.91**	**−1.92**
Parkin RBR E3 ubiquitin protein ligase (PARK2)	**−2.24**	**−2.77**
Platelet factor 4 (PF4)	**−2.94**	**−2.91**
Phospholipase A2 group IIA (PLA2G2A)	**−2.83**	**−2.76**
Phospholipase C-like 2 (PLCL2)	NS	−1.59
Pleckstrin homology domain containing B1 (PLEKHB1)	**−1.97**	**−2.14**
Protein kinase C, theta (PRKCQ)	NS	−1.62
Similar to RIKEN cDNA 1300017J02 (RGD1310507)	NS	−2.48
Butyrophilin-like 10 (RGD1559732)	−4.38	NS
Regulator of G-protein signaling 18 (RGS18)	NS	−2.15
Rh-associated glycoprotein (RHAG)	−3.61	NS
Rh blood group, D antigen (RHD)	−3.76	NS
RIO kinase 3 (RIOK3)	−1.53	NS
Radical S-adenosyl methionine domain containing 2 (RSAD2)	**−4.82**	**−4.94**
RT1 class Ib, locus S2 (RT1-S2)	−4.82	NS
Serpin family B member 11 (SERPINB11)	**−4.76**	**−3.01**

Inhal Toxicol. Author manuscript; available in PMC 2023 November 20.

Transcript	Fold change Acute	in expression Sub-chronic
S100 calcium binding protein A8 (S100A8)	NS	−1.65
Solute carrier family 2 member 4 (SLCA4)	NS	−3.54
Solute carrier family 25 member 37 (SLC25A37)	−1.65	NS
Solute carrier family 25, member 39 (SLC25A39)	−2.38	NS
Spermine oxidase (SMOX)	**−1.68**	**−1.69**
Spectrin, alpha, erythrocytic 1 (SPTA1)	−3.38	NS
Transcription factor Dp-2 (TFDP2)	NS	−1.56
Tubulin, beta 1 class VI (TUBB1)	**−2.68**	**−2.97**
UBA domain containing 1 (UBAC1)	−1.84	NS
Yippee-like 5 (YPEL5)	**−1.81**	**−1.92**

Genes with a significant differential expression (FC > 1.5 and FDR $p<0.05$) in the acute or sub-chronic exposure group at the 28-d post-exposure interval are presented. There were 30 SDEGs common between the two groups which are presented in bold. NS - Not significantly different based on the selection criteria (>1.5-fold change in expression and FDR, $p<0.05$).